Light-Induced Voltage Noise in the Photoreceptor of *Drosophila melanogaster*

CHUN-FANG WU and WILLIAM L. PAK

From the Department of Biological Sciences, Purdue University, West Lafayette, Indiana 47907. Dr. Wu's present address is the Division of Biology, California Institute of Technology, Pasadena, California 91125.

ABSTRACT   The *Drosophila* photoreceptor potential is thought to be composed of discrete unit potentials called bumps. The steady-state receptor potential and the accompanying voltage fluctuations were recorded intracellularly under steady illumination. The occurrence rate, effective amplitude, and duration of the bumps were deduced by assuming a shot noise model. Over a wide range of light intensity, the duration of bumps remained essentially constant (25–30 ms). Below the saturation intensity for the receptor potential, the bump rate was roughly proportional to the intensity, and the adjustment of bumps to smaller size at higher intensity was mainly responsible for the nonlinear behavior of the receptor potential. The reduction in the size of bumps at increasing light intensity was found to be due mainly to the diminishing magnitude of the bump current, and not to some other secondary effects. The bump rate saturated at about 3×10^5–10^6 events/s.

INTRODUCTION

The electrical signals of many biological membrane systems arise from the summation of unitary conductance changes. Shot noise analysis has been widely applied to study these elementary conductance events (Adolph, 1964; Hagins, 1965; Dodge et al., 1968; Katz and Miledi, 1972; Anderson and Stevens, 1973; Conti et al., 1975). In the case of several arthropods studied, small, discrete potentials, or "quantum bumps," have been recorded from the dark adapted photoreceptor cells (Yeandle, 1957; Adolph, 1964; Scholes, 1965; Kirschfeld, 1966). It is thought that these bumps superimpose to form the receptor potential (Rushton, 1961; Fuortes and Yeandle, 1964; Dodge et al., 1968). Under steady stimulus conditions, however, individual bumps cannot be readily recognized. Instead, the receptor potential is often accompanied by prominent noise fluctuations. On the basis of shot noise analysis, Dodge et al. (1968) have shown in *Limulus* that the frequency response of the receptor potential could be predicted from the characteristics of the noise fluctuations. Their findings thus suggested that the fluctuations originated from the random summation of the elementary shots (bumps) comprising the receptor potential. Furthermore, the occurrence rate and the effective amplitude of the bumps at different light intensities could be computed from the mean amplitude of the receptor potential and the variance of the accompanying fluctuations. From such

calculations it was found that the unitary bumps are strongly light-adapted to smaller size. In fact, this light-induced decrease in the size of unitary bumps is thought to be the main cause of adaptation in the receptor potential (Dodge et al., 1968). The light and dark adaptation properties of quantum bumps have also been studied with weak test stimuli which allow identification of individual bumps (Adolph, 1964; Srebro and Behbehani, 1972; Fein and Charlton, 1975). The results of such studies have led to conclusions similar to those obtained with stronger stimuli.

Quantum bumps have also been found to occur in the *Drosophila* retinula cells and have been shown to be the elementary units of the receptor potential, independent of stimulus wavelength (Wu and Pak, 1975). As in the case of *Limulus*, the frequency response of the receptor component of the *Drosophila* electroretinogram could be deduced from the power spectrum of the intracellularly recorded receptor noise (Wu and Wong, 1977). Thus, it seemed worthwhile to examine the parameters and kinetics of the bumps in *Drosophila* under different light conditions, in the hope that the behavior of the receptor potential may be inferred from the bump properties. Shot noise analysis has been applied in the present study to obtain the duration, amplitude, and occurrence rate of bumps underlying the steady-state receptor potentials.

The genetic approach to the problem of phototransduction using *Drosophila* mutants has provided useful information which is difficult to obtain by other means (Alawi et al., 1972; Minke et al., 1975a; Pak, 1975; Pak et al., 1976). Inasmuch as quantum bumps are the first signs of electrical response to light stimulation, alterations in the transduction process are likely to be reflected in the bump parameters. For example, there may be marked differences in the rate (Minke et al., 1975a) and the latency distribution (Pak et al., 1976) of bump production in phototransduction mutants. Therefore, knowledge of bump properties in the normal *Drosophila* photoreceptors is important in furnishing the basis for further studies on phototransduction mutants. Thus, another reason for undertaking the present studies was to provide such baseline data on the normal photoreceptors.

METHODS

Fruitflies *Drosophila melanogaster* bearing the sex-linked recessive mutation white (w) (Lindsley and Grell, 1968) were used throughout the experiments to eliminate the effects of the screening pigments and pigment granule migration (Alawi et al., 1972; Wu and Wong, 1977). The preparation and techniques for intracellular recordings have been described in a previous paper (Wu and Pak, 1975). The glass capillary microelectrodes were filled with 2 M KCl. The electrode resistance varied from about 80 to 150 MΩ when measured in physiological saline. The stimulus originated from a 150 W xenon arc lamp forming the light source for a high intensity monochromator (Bausch and Lomb Inc., Analytical Systems Div., Rochester, N. Y.). The unattenuated illuminance at the level of the preparation was 3.6×10^{14} photons/cm² per s at 540 nm (half-peak bandwidth of 16 nm). The stimulus durations varied between about 30 s and 1 min. These durations were chosen so as to allow sufficient lengths of records to be collected at various light intensities. Between light stimuli, the preparation was allowed to dark adapt for 30–120 s, depending on the previous stimulus intensity. Voltage signals were picked up by an M4A electrometer (W-P Instruments, Inc., New Haven, Conn.) and displayed on an oscillo-

scope and a brush pen recorder (Gould Inc., Instrument Systems Div., Cleveland, Ohio). The signals were also stored on magnetic tape, which accepted a frequency band from zero to 1000 Hz.

The autocovariance function $C(\tau)$ of the steady-state component of the receptor potential was computed according to the formula

$$C(\tau) = \overline{\{v(t) - \bar{v}\}\{v(t + \tau) - \bar{v}\}}, \tag{1}$$

where $v(t)$ is the voltage at time t, τ is the time lag, and the bars represent time averages. The mean steady-state response $\bar{v}$ is defined here with respect to the voltage baseline obtained after prolonged dark adaptation. The calculation was based on 750 points sampled at 8-ms intervals. A Hewlett-Packard 9864A digitizer and a 9830A calculator (Hewlett-Packard, Palo Alto, Calif.) were used to sample and compute the data. The whole system for recording and data processing was calibrated by sine waves of known frequency.

For measuring the reversal potential of the photoresponse, steady currents were applied through the recording electrode. The potential drop due to the electrode resistance was balanced out using a bridge circuit built into the W-P Instruments electrometer. Electrodes of relatively low resistances (80–120 MΩ) were chosen for this purpose to insure that the bridge circuit reliably balanced out the electrode resistance. The resistance of electrodes was checked in tissue both before penetration and after withdrawal from the cell. The amount of current injected through the electrode was usually <1 nA, and the electrode resistance measured in saline remained essentially constant in this range. In addition to steady current injection, the membrane resistance was also measured by applying current pulses and recording the voltage response of the membrane with the bridge circuit. Both methods gave similar results.

The observed amplitude of the bump noise varied from cell to cell, presumably due to different recording sites within the photoreceptor. The bump noise is usually strongly attenuated if the recording electrode is positioned at the retinula cell axon, away from the signal source in the soma (Zettler and Järvilehto, 1973). Only the cells which exhibited prominent bump noise were selected for the analyses reported here. Because of the small cell size, only a small percentage (~5%) of the penetrated cells gave stable enough recordings and had large enough bump noise to meet our selection criteria.

RESULTS

Qualitative Observations

Fig. 1 illustrates a typical receptor potential with accompanying noise fluctuations under conditions of increasing light intensity. The steady-state amplitude of the receptor potential increases with light intensity and becomes saturated at high light levels, reaching about half the maximum amplitude of the initial transient peak. No spikes have been observed at any phase of the receptor potential. As shown in Fig. 1, the magnitude of noise first increases with light stimulus ($\log I = -4$ and -3), passes through a maximum, and then declines gradually ($\log I = -2$, -1 and 0) to level off at high intensities ($\log I = -1$ and 0). At saturating light intensities, the receptor potential still retains noise fluctuations substantially above the dark level ($\log I = 0$, Fig. 1).

Shot Noise

Let us suppose that the steady-state receptor potential is made up of randomly occurring bumps (elementary shots). Except at very low stimulus intensities,

individual bumps generally are not recognizable, and the presence of bumps manifests itself only as noise superimposed on the receptor potential. Even under such conditions, the properties of bumps may be deduced using Campbell's theorem (Rice, 1944). According to Campbell's theorem, the mean receptor potential amplitude $\bar{v}$ and the associated noise variance s^2 can be related
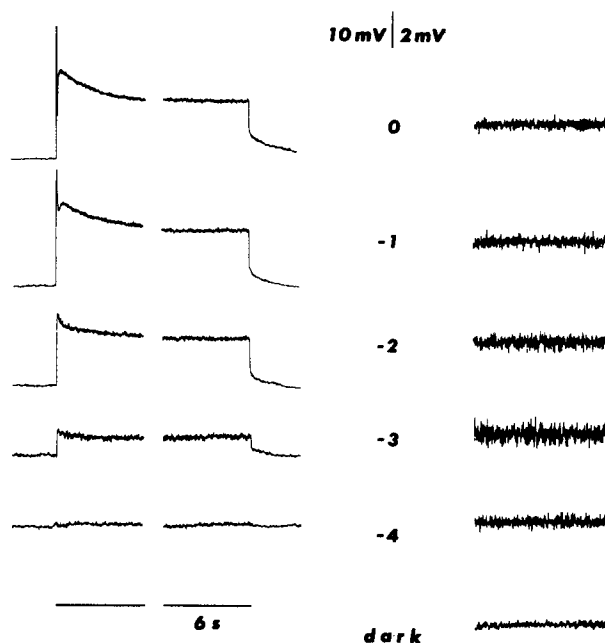

FIGURE 1. The receptor potentials with accompanying noise fluctuations under conditions of increasing light intensity. The transient phase and the steady-state phase of the receptor potential are shown on the left. The lines below the responses indicate the duration of stimulus. The noise fluctuations recorded during the steady-state response and in darkness are shown on the right in higher amplification. Numbers indicate relative intensities of stimuli (540 nm) in log units. Time calibration applies to all traces in the figure.

to the occurrence rate n and the time-course $f(t)$ of the bump[1] by the following equations:

$$\bar{v} = n \int_0^\infty f(t) \, dt, \tag{2}$$

$$s^2 = \overline{(v(t) - \bar{v})^2} = n \int_0^\infty f^2(t) \, dt. \tag{3}$$

Computations of Eqs. 2 and 3 can be greatly simplified by utilizing the concepts of "effective" shot amplitude a and duration T, defined by the following expressions (Knight, 1972):

---

[1] If the size of shots varies, $f(t)$ represents the time-course of the shot having the mean size, and Eqs. 2 and 3 still hold (Rice, 1944).

$$a = \frac{\int_0^\infty f^2(t)\, dt}{\int_0^\infty f(t)\, dt},$$ (4)

$$T = \frac{\left(\int_0^\infty f(t)\, dt\right)^2}{\int_0^\infty f^2(t)\, dt}.$$ (5)

For idealized rectangular shots with amplitude a and duration T, these expressions are clearly true, while for other shot shapes they may serve as definitions of the "effective" amplitude and duration. By direct substitution of Eqs. 4 and 5 into Eqs. 2 and 3, Campbell's theorem reduces to

$$\bar{v} = naT,$$ (2.1)

$$s^2 = na^2T,$$ (3.1)

where aT is equal to the area under each bump $\int_0^\infty f(t)\, dt$. The effective amplitude a may be readily computed from Eqs. 2.1 and 3.1:

$$a = \frac{s^2}{\bar{v}},$$ (6)

where the mean voltage $\bar{v}$ and the noise variances s^2 of the receptor potential are experimentally measurable quantities.

The noise observed during illumination contains both the noise induced by light and the "dark noise" which occurs steadily both in the dark and during illumination. If one assumes, however, that the noise in the dark and the light-induced noise are independent of each other, the variance s^2 of the light-induced noise can be obtained as the difference between the variance s_o^2 of the noise observed during illumination and the dark noise variances s_d^2, i.e.,

$$s^2 = s_o^2 - s_d^2.$$ (7)

If the effective duration T is known at various light intensities, the shot rate n and the effective amplitude a can be computed from Eqs. 2.1 and 3.1 for any given mean response amplitude $\bar{v}$ and noise variance s^2. Moreover, the effective duration T can be deduced from the noise characteristics of the voltage fluctuations during steady illumination (Dodge et al., 1968). Thus information about the shot rate n and effective amplitude a can be obtained even though individual shots are not recognizable.

Temporal Characteristics of the Potential Fluctuations

The temporal characteristics of a stationary shot noise process, i.e., one whose statistical properties do not change with time, are given by its autocovariance function

$$C(\tau) = \overline{\{v(t) - \bar{v}\}\{v(t + \tau) - \bar{v}\}},$$ (1)

where τ is the time lag. Thus $C(0)$ is the variance of the noise s^2 (Eq. 3), and $C(\tau)$ at $\tau \neq 0$ gives a picture of how the signal is correlated with what it will be at τ-interval in the future, or what it was at τ-interval in the past. When the shots are uncorrelated, or randomly occurring, $C(\tau)$ is determined by the time-course of the elementary shots only. From the same steady-state responses shown in Fig. 1, the autocorrelation functions at different light intensities have been computed for the *Drosophila* photoreceptor using Eq. 1. A sample of the results, normalized to $C(0)$, is shown in Fig. 2. The autocovariance $C(\tau)$ declines to smaller values as τ increases. A 1,000-fold increase in light intensity makes the decline of $C(\tau)$ slightly more rapid, consistent with the finding in the *Limulus* lateral eye (Dodge et al., 1968). However, the effect of increasing light intensity is much smaller in *Drosophila* than in *Limulus*. In all eight cells studied, an increase in light intensity did not seem to alter the autocovariance function of the *Drosophila* steady-state
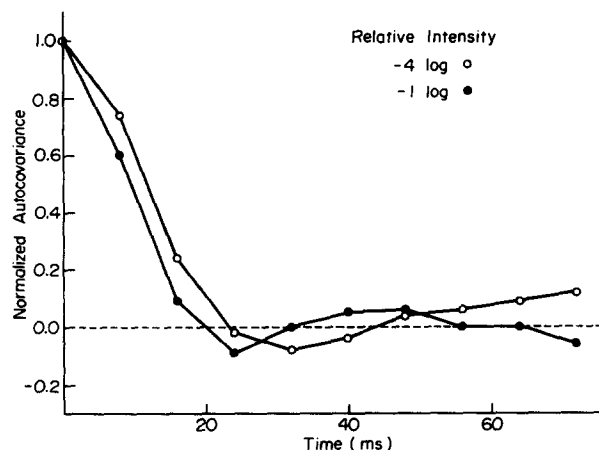

FIGURE 2.   Normalized autocovariance functions of the steady-state response measured at two light intensities. Same cell as in Fig. 1.

response appreciably. Inasmuch as in the case of uncorrelated bumps $C(\tau)$ is determined by the time-course of the bumps only, the above results suggest that the time-course of the bumps remains essentially constant over the range of intensities tested. The light intensity appeared to have a much stronger effect on the rate n and the effective amplitude a (see Fig. 4).

Assuming that the bumps are uncorrelated, the autocovariance function $C(\tau)$ has been used to estimate the effective duration T of bumps (Wong, 1977), as shown below. The expression for the autocovariance function (Eq. 1) may be rewritten in terms of the time-course of the bump $f(t)$:

$$C(\tau) = n \int_0^\infty f(t)f(t + \tau)\, dt, \tag{1.1}$$

where the symbols have been defined previously.[2] Using this expression, the area under the normalized autocovariance function can be shown to be the effective duration T (Eq. 5) of a shot having the time-course $f(t)$:

[2] For derivation, see Rice, 1944, p. 172.

$$\int_{-\infty}^{\infty} C(\tau)/C(0) \, dt = \left[\int_{-\infty}^{\infty} \int_{-\infty}^{\infty} f(t)f(t + \tau) \, dt \, d\tau \right] \Big/ \int_{-\infty}^{\infty} f(t)f(t) \, dt$$

$$= \left[\int_{0}^{\infty} f(t) \, dt \right]^{2} \Big/ \int_{0}^{\infty} f^{2}(t) \, dt. \tag{5.1}$$

Thus, the effective bump duration T was obtained by integrating the normalized autocovariance curves in Fig. 2 and was found to be approximately 25–30 ms.

Mean Amplitude and Standard Deviation of the Steady-State Response

Five cells showing prominent noise fluctuations and yielding long, stable recordings have been selected for the following analysis. The observed steady-state response amplitudes were normalized to that of the saturated response and plotted against relative log intensities in Fig. 3 A. The data points could be fitted by the function

$$\frac{\bar{v}}{\bar{v}_{\max}} = \frac{I}{I + \sigma}, \tag{8}$$

where $\bar{v}$ is the mean amplitude of the steady-state response[3] at any given light intensity I, $\bar{v}_{\max}$ is the maximum attainable $\bar{v}$, and σ is the intensity which evokes $1/2 \, \bar{v}_{\max}$ (Naka and Rushton, 1966). In the cells reported here, log σ ranged from -2.5 to -3.2. In that we are dealing with relative intensities, the units of intensity in Fig. 3 have been chosen so that σ is equal to 1 (log $\sigma = 0$). The standard deviation s of the light-induced noise was normalized with respect to the maximum value obtained in the same cell and is plotted against relative light intensities in Fig. 3 B. In the five cells analyzed, the magnitude of $\bar{v}_{\max}$ ranged from 9 to 16 mV and the maximum standard deviation varied from 0.20 to 0.34 mV.

At low light intensities, the rate of bump production n is known to increase in proportion to light intensity (Adolph, 1964; Fuortes and Yeandle, 1964; Scholes, 1965; Wu and Pak, 1975). A question of some importance is whether this linear relationship is maintained at high light intensities where individual bumps are no longer recognizable. The mean steady-state response $\bar{v}$ is linear only in a very restricted intensity range, where I is much smaller than σ, and becomes saturated when I is much greater than σ. In order to explain the nonlinearity, either the effective amplitude a or shot rate n (or both) must decrease under conditions of increasing light intensity, because T has been shown to be relatively constant.

Let us first assume that the rate n is strictly proportional to the light intensity, i.e., $n = k_1 I$ where k_1 is a constant, and see if a change in the effective amplitude a alone could explain the observed nonlinearity in the steady-state response $\bar{v}$ and the accompanying standard deviation s. Before treating the effective amplitude a as a variable, consider a simple linear model in which a is a constant

---

[3] In contrast to the steady-state response, the initial transient peak v_p is best fitted by a function of the form:

$$v_p/v_0 = I^{0.5}/(I^{0.5} + \sigma^{0.5}),$$

where v_0 is the maximum attainable peak amplitude (Minke et al., 1975b).

and the shots summate linearly. It is evident that the mean summated voltage $\bar{v}_1$ derived from this model is proportional to the intensity I, i.e.,

$$\frac{d\bar{v}_1}{dI} = k_2, \tag{9}$$

where k_2 is a constant. From Eq. 3.1 the light-induced noise variance s_1^2 in the linear model is proportional to the intensity I, i.e.,

$$s_1 = k_3 I^{1/2}, \tag{10}$$

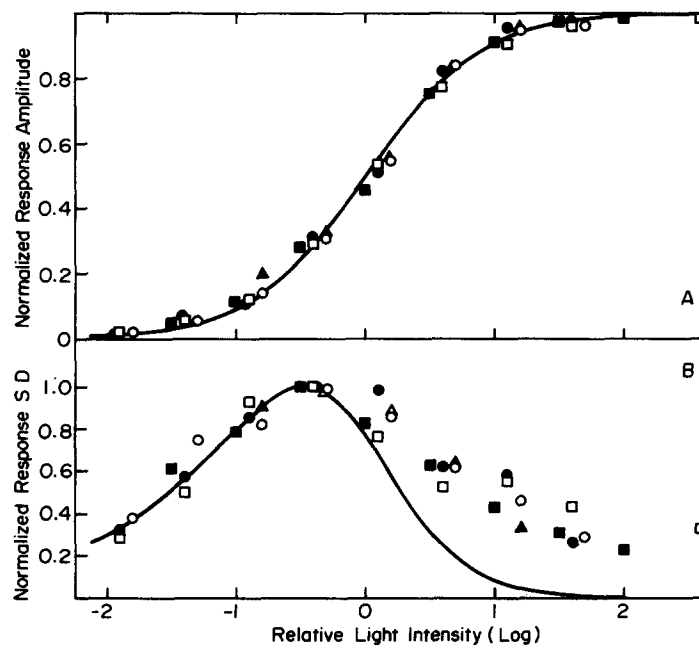where k_3 is another constant.

FIGURE 3. Mean amplitude and noise standard deviation of the steady-state response as functions of light intensity. Data obtained from five cells are plotted against the relative light intensity. The units of intensity have been chosen so that σ, which evokes $^{1}/_{2}\ \bar{v}_{max}$, is equal to 1 ($\log \sigma = 0$). (A) Mean amplitudes normalized to the saturated response amplitude of the same cell. (B) Noise standard deviations (SD) normalized to the maximum standard deviation recorded in the same cell. The curves in (A) and (B) are computed from Eqs. 8 and 14, respectively.

However, this simple linear model obviously cannot account for the nonlinear dependence of the mean steady-state receptor potential $\bar{v}$ on the light intensity I described by Eq. 8. As I increases, the true mean receptor potential $\bar{v}$ becomes progressively smaller than $\bar{v}_1$ of the linear model (Eq. 9). The same is true for the relationship between the noise standard deviation s and that of the linear model, s_1 (Eq. 10).

To account for the nonlinear properties of the mean receptor potential $\bar{v}$, we

now proceed to derive the relation between the noise standard deviation s and the intensity I under the condition that only the effective amplitude a varies with the light intensity I. The rate n is again taken to be strictly proportional to I. For relatively small fluctuations about the means $\bar{v}$ and $\bar{v}_1$, such as the standard deviations s and s_1,

$$s = s_1 \frac{\mathrm{d}\bar{v}}{\mathrm{d}\bar{v}_1}. \tag{11}$$

Therefore, using the chain rule,

$$s = s_1 \frac{\mathrm{d}\bar{v}}{\mathrm{d}I} \cdot \frac{\mathrm{d}I}{\mathrm{d}\bar{v}_1}. \tag{12}$$

Eq. 8 may be rewritten

$$\bar{v} = \bar{v}_{\mathrm{max}} \frac{I}{I + 1}, \tag{8.1}$$

and

$$\frac{\mathrm{d}\bar{v}}{\mathrm{d}I} = \bar{v}_{\mathrm{max}} \frac{1}{(I + 1)^2}, \tag{13}$$

where the units of the relative intensity have again been chosen so that $\sigma = 1$. Substituting Eqs. 9, 10, and 13 into Eq. 12, we have

$$s = \mathrm{constant} \cdot \frac{I^{1/2}}{(I + 1)^2}. \tag{14}$$

Eq. 14 describes the relationship between the noise standard deviation s and the intensity I if the rate n is strictly proportional to I and if the change of the bump amplitude is solely responsible for the nonlinear behavior of the receptor potential. (Recall that the effective duration T is a constant.)

In Fig. 3 B, Eq. 14 is plotted against the observed standard deviations of light-induced noise. The calculated noise standard deviation s increases with I at lower light intensities. The magnitude of s passes through a maximum at $I = \frac{1}{3} \sigma$ ($\sigma = 1$ in Eq. 14) and then declines gradually towards zero. Eq. 14 fits the observed noise standard deviation at low and intermediate light intensities. However, the observed s remains relatively constant at high intensities, instead of declining towards zero. Since at low intensities the rate n is known to be proportional to light intensity I, the results shown in Fig. 3 B indicate that the linear relationship between n and I seen at lower light intensities is not maintained at high light intensities.

Relative Rates and Effective Amplitudes of Bumps at Different Intensities

The same data plotted in Fig. 3 have been used to compute a and nT directly from Campbell's theorem (Eqs. 2.1 and 3.1), and without correcting for nonlinearity between conductance and voltage, the values of a and nT so obtained are plotted in Fig. 4 as functions of light intensity. The quantity nT may be regarded as the rate n given in relative units, since T is approximately
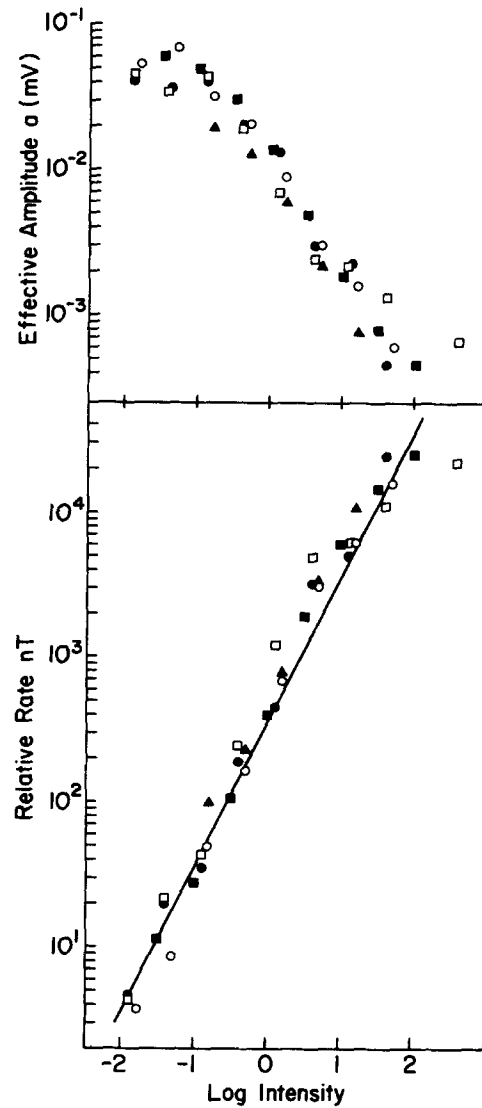
FIGURE 4. Dependence of effective amplitude a and rate of bump product nT on the relative light intensity. The units of intensity were chosen so as to make σ equal to 1 (log σ = 0). The same data presented in Fig. 3 were used to calculate a and nT from Eqs. 2.1 and 3.1. The quantity nT may be regarded as the rate n given in dimensionless, relative units, since the effective duration T is approximately constant. A straight line corresponding to a first power relation (real slope of 1) is fitted to the data points at intensities below σ (log I < 0). (Because the vertical log scale is expanded to twice the horizontal scale, the above line has a ruler-measured slope of 2.) The effective duration T was estimated to be about 25-30 ms. Thus, one nT corresponds to an absolute rate of 30-40 events/s.

constant. In absolute terms, one nT would correspond to n of 30–40 bumps/s, since T is approximately 25–30 ms. Note that the intensity scale in Fig. 4 is drawn relative to the half-saturation intensity σ (log σ = 0). Thus, for each cell from which recordings were made, the data points were plotted with respect to σ of that cell. No other attempts were made to either scale or normalize the data. The effective amplitude a shows some scatter because the observed noise amplitude varied slightly from cell to cell despite the rigid criteria applied to the selection of cells (see Methods). As to be discussed shortly, the same data have been corrected for nonlinear summation of bumps and are presented in Fig. 6. However, we first consider the uncorrected data.

As shown in Fig. 4, the bump rate n increases with rising intensity. A line of slope 1 (first power relation) is fitted to the data points at intensities below σ (log I < 0). A linear regression analysis on these data points (log I < 0) gave a slope of 1.07 ± 0.13 (SE of slope) with a correlation coefficient of 0.98. For intensities higher than σ, there is a region where n rises more steeply than 1. The slope of the regression line for the data points at intensities $0 \leq \log I < 1$ was computed to be 1.35 ± 0.14. The rate n apparently levels off in the saturation intensity region (log $I \geq 1$). The slope of the regression line for the points in this region was 0.45 ± 0.14. The effective amplitude a, on the other hand, remains relatively constant at low intensities (log I < −1.0) and then becomes light-adapted to smaller amplitude with increasing intensity. At sufficiently high intensities, a also shows a tendency to saturate.

Reversal Potential of the Light Response

There are several possible mechanisms which could be responsible for the decrease in the effective bump amplitude at higher light intensities. One possible explanation is that as light intensity increases, the steady-state receptor potential $\bar{v}$ gradually approaches the equilibrium potential of the ion species responsible for the receptor potential. Therefore, the observed voltage change due to each additional increment in membrane conductance is progressively reduced. To correct for the effect of such nonlinear summation, the reversal potential of the photoreceptor response has been measured by applying steady polarizing currents through the recording electrode. The potential drop due to the electrode resistance was balanced out by means of a bridge circuit (see Methods). Measurements were made only when the penetrated cells exhibited large bump noise, indicating a recording site near the signal source.

Fig. 5A shows a sample of records. Hyperpolarizing currents increased the size of response to light and depolarizing currents reduced it. At sufficiently high current magnitudes, depolarizing currents reversed the polarity of response. The current-voltage relationships obtained from the same cell in dark and during light are plotted in Fig. 5B. Two straight lines have been fitted to the data points. The slopes of the lines correspond to the cell membrane resistances. The membrane resistance decreased from about 32 MΩ in darkness (●) to about 18 MΩ during light response (O). The lines intersected at a reversal potential of 27 mV above the resting level in this cell.
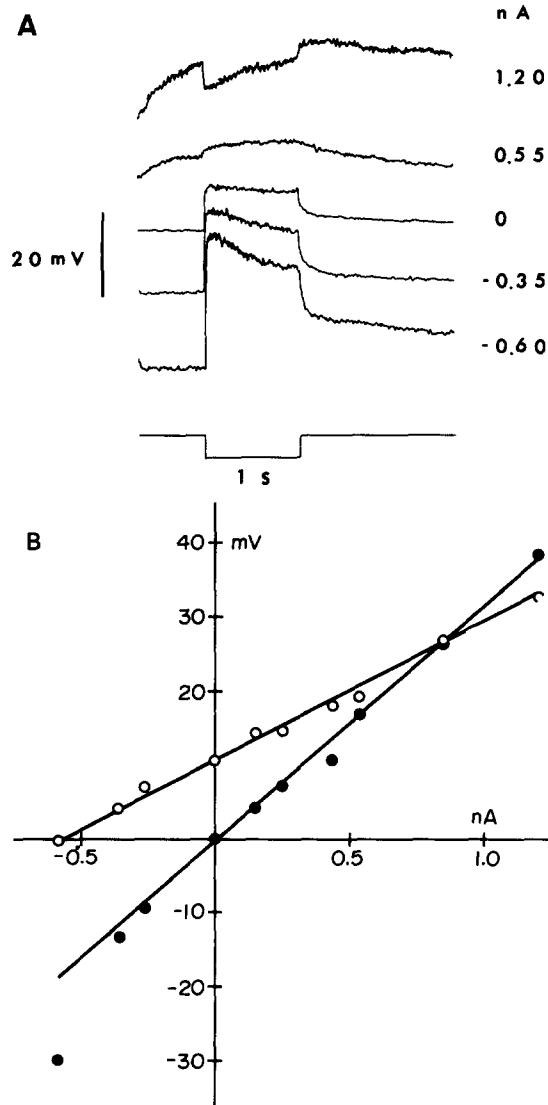
FIGURE 5. Effect of steady currents on the photoreceptor potential. (A) Records of receptor potentials during passage of steady currents. Positive numbers indicate the strengths of depolarizing currents and negative numbers the strengths of hyperpolarizing currents. Traces begin immediately after the onset of current injection. Currents were applied through the recording electrode, and the potential drop due to the electrode resistance was balanced out by a bridge circuit. The downward deflection in the bottom trace indicates the duration of light stimulus (540 nm, log $I = -2$). (B) Current-voltage relations in darkness and at peak of response to light. Data from the same cell as in (A) are plotted. (●), displacements of membrane potential caused by currents of different strengths in darkness. (○), peak response to light during application of currents. Two straight lines are fitted to the data points. The membrane resistance (slope of the straight line) decreases from 32 MΩ in darkness to about 18 MΩ during light response. The lines intersect at a reversal potential of 27 mV above the resting potential in this cell.

In seven cells yielding stable current-voltage characteristics, the reversal potential was 32.1 ± 7.0 mV (mean $\pm$ SD) above the resting potential. The resting potential, measured in 26 cells, was found to be -27.0 ± 4.7 mV (mean $\pm$ SD) with respect to the extracellular medium. The maximum amplitudes the receptor potentials can attain at high stimulus intensities have also been measured. In 16 cells, the maximum attainable depolarization at the transient peak was 28.6 ± 5.1 mV, and the maximum steady-state amplitude was 15.4 ± 3.6 mV above the resting level. Thus, the maximum value the steady-state phase of the receptor potential ($\bar{v}_{max} = 15.4 \pm 3.6$ mV) can attain is only about half the reversal potential level (32.1 ± 7.0 mV) when measured from the resting potential level. Therefore, the steady-state potential never approaches the reversal potential closely enough to substantially affect the bump amplitude. In fact, if $\bar{v}_{max}$ is about half the reversal potential, the voltage change due to a given conductance change is expected to decrease by a factor of no more than two as $\bar{v}$ approaches $\bar{v}_{max}$ (Martin, 1966).

Corrections for Nonlinear Summation of Bumps

We have corrected for nonlinear summation of bumps due to variations in the mean steady-state response, $\bar{v}$, using a simple resistive equivalent circuit for the membrane (Katz and Miledi, 1972). The maximum steady-state response $\bar{v}_{max}$ was assumed to be one-half of the reversal potential.

In Fig. 6, the corrected values of the effective amplitude a and relative rate nT are plotted against the relative light intensity (log $\sigma = 0$). In comparison to the uncorrected data (Fig. 4), the linear region of the corrected bump rate nT extends to a higher light intensity. A line of first power relation (slope 1) was fitted to the data points in the intensity region log $I \leq 1$ (Fig. 6). A linear regression analysis on these data points (log $I \leq 1$) yielded a slope of 0.96 ± 0.13 (SE) with correlation coefficient of 0.99. Again the rate tends to saturate above log $I = 1$. The relative rate nT has been converted to absolute bump rate, taking the effective duration T to be 28 ms. The absolute rate scale so obtained is indicated on the right hand side of Fig. 6. The bump rate appears to saturate at about 3×10^5 events/s. In contrast, the uncorrected results in Fig. 4 indicate that the rate saturates at about 10^6 events/s.

The effective amplitude a decreases monotonically as light intensity increases (Fig. 6). It, however, decreases by less than two orders of magnitude over an intensity range of more than 4 log units.

Since the correction procedure we adopted tends to result in overcorrection (Stevens, 1976), the corrected results (Fig. 6) may be regarded as the lower limit for n and upper limit for a, respectively, while the uncorrected results (Fig. 4) may be regarded as the upper and lower limits for n and a, respectively (see Discussion).

DISCUSSION

Sources of Error

Several factors could contribute to error in estimating the effective amplitude and rate of bumps. Error can be introduced by the presence of synaptic feedback from secondary neurons to the receptors and lateral interactions at

the receptor level. Such synaptic activities would not only change the mean receptor potential amplitude but also the noise level. However, electron microscopic observations do not provide evidence for the existence of such lateral and feedback synapses in the compound eye of muscoid flies (Trujillo-Cenóz, 1965; Boschek, 1971). Moreover, the transient hyperpolarization at light-off, which
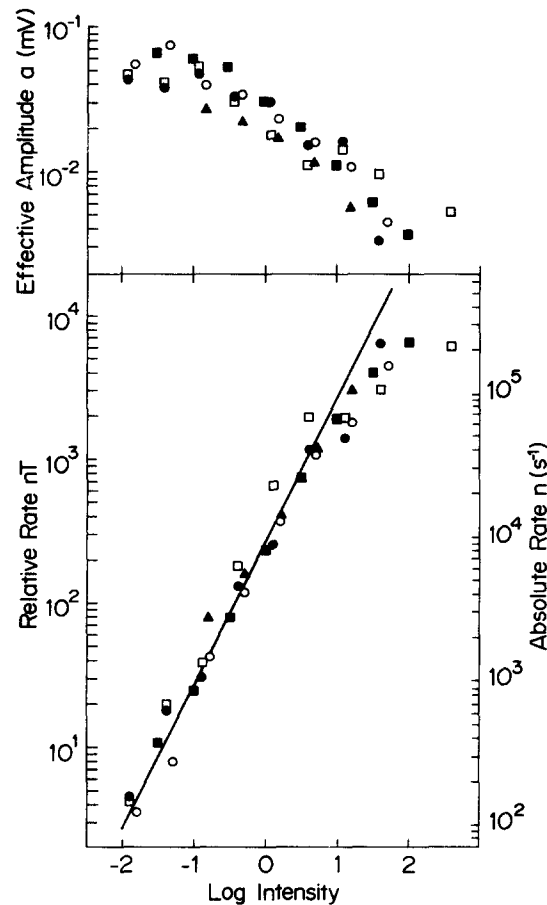

FIGURE 6. Intensity dependence of effective amplitude and rate corrected for nonlinear summation. Same data as in Figs. 3 and 4. A line of first power relation (slope 1) is fitted to the data points of rate in the intensity region $\log I \leq 1$. Indicated along the vertical axis on the right hand side is the scale for absolute bump rate n obtained from nT by taking the effective duration T to be 28 ms.

has been correlated with synaptic feedback in the dragonfly ocellus (Dowling and Chappell, 1972), was not present in the preparations used in this study. In addition, since synaptic activities are expected to occur near the receptor axon terminals, the synaptic signals are likely to be strongly attenuated by the time they reach the recording site in the soma (see Methods, and also Zettler and Järvilehto, 1973). Thus, even if such synapses were present in the Drosophila compound eye, their contribution to error probably is not serious.

Another source of error is the electrical coupling between receptor cells. Extensive coupling can reduce the amplitude of the quantal noise, as reported in the toad (Fain, 1975) and the turtle (Simon et al., 1975). Coupling among retinula cells has been observed in several arthropod species with fused rhabdoms, such as *Limulus* (Smith et al., 1965), the honeybee (Shaw, 1969) and the crayfish (Muller, 1973). However, in all these cases the coupling appears to be restricted to the same ommatidia, and the effect of coupling is much smaller than that found in vertebrates. In any case, to our knowledge no evidence for coupling between photoreceptors has yet been found in the dipteran eye. Indeed, behavioral studies indicate that each retinula cell in the ommatidium functions independently in the open-rhabdom eyes of muscoid flies (Kirschfeld, 1972).

The measurements of the membrane resistance and the reversal potential for the photoresponse showed considerable variability. Some uncertainty could be introduced because the same electrode was used to both record the responses and pass polarizing currents. The electrode resistance was assumed to be constant throughout the measurement. However, the electrode resistance may vary with the amount of current passing through the tip and with the medium in which the tip is immersed. Therefore, the value of the electrode resistance when the tip is inside the cell cannot be precisely determined. In addition, because of the long, cylindrical shape of the retinula cell, it is virtually impossible to obtain isopotential conditions inside the cell when polarizing currents are applied.

However, the following consideration suggests that the kinds of errors discussed above probably are not serious. Using larger arthropod photoreceptors in which the reversal potential could be determined much more reliably by means of separate current and voltage electrodes, other investigators (Millecchia and Mauro, 1969*a, b*; Brown et al., 1970) have shown that the initial transient of the receptor potential approaches the reversal potential at high stimulus intensities. We also found that at high intensities the transient peak of the *Drosophila* receptor potential (28.6 $\pm$ 5.1 mV) attains values close to the observed reversal potential (32.1 $\pm$ 7.0 mV). A t test showed no significant difference between the mean amplitude of the transient peak and the mean reversal potential at the level of 0.05 ($t = 1.35, df = 21$). Moreover, as may be seen in Fig. 5A, the transient peak and the steady-state phase of the receptor response seem to have nearly the same reversal potential, consistent with findings in other arthropods. Thus, our findings on the reversal potential of *Drosophila* photoreceptors are both qualitatively and quantitatively similar to those on larger arthropod photoreceptors, in which separate current and voltage electrodes were used.

Error would also arise if the photoreceptor response is composed of more than one type of ionic process. Fig. 1 shows that, after the light-off, the voltage response returns to the base line in two stages. If the slow second component does not consist of light-induced bumps, this component would have to be excluded in calculating the mean steady-state response, $\bar{v}$. However, there is no a priori reason to believe that the slower component does not consist of bumps. In fact, it is likely to be related to the prolonged depolarizing afterpotential

(PDA) (Minke et al., 1975b), which is thought to consist of random shots similar to light-induced bumps (Minke et al., 1975a). Thus, in the absence of information to the contrary, we have treated both components of the photoreceptor response to consist of bumps and defined $\bar{v}$ accordingly.

The light-induced noise was obtained by taking the difference between the noise variances observed during illumination and those in darkness (Eq. 7). The dark noise contains spontaneous bumps in addition to the background noise (Wu and Pak, 1975). Under light-adapted conditions, the spontaneous bumps, if still present, might be much smaller than under dark-adapted conditions. If so, Eq. 7 would tend to underestimate the variance s^2 of the light-induced noise and, hence, underestimate the effective bump amplitude a (Eq. 6) and overestimate the rate (Eq. 2.1) for any given value of the mean steady-state response $\bar{v}$. Although the rate of spontaneous bumps is low ($nT \simeq 0.2$–0.3, computed from the data in Wu and Pak, 1975), the error may be appreciable at saturating light intensities where light-induced noise is also small. The variance due to spontaneous bumps in the dark ($s_a{}^2$) is about 0.001–0.002 mV^2, while the corrected noise variance during saturated steady-state receptor potential (s^2) is about 0.007 mV^2. Thus, if the spontaneous bumps also light-adapted to smaller size, the error from this source could be 10–20%.

Several methods have been devised to correct for the nonlinear relationship between the voltage and conductance across the cell membrane (Martin, 1966; Katz and Miledi, 1972; Stevens, 1976). Corrections based on simple resistive equivalent circuits, which we have adopted, are usually not entirely satisfactory and lead to overcorrection (Stevens, 1976). Moreover, the exact function for correcting nonlinearity depends on several factors, e.g., the membrane capacitance and the time course of conductance change, which are difficult to determine experimentally (Stevens, 1976).

Recently, Wong and Knight (1977) have measured the bump parameters from the Limulus ventral eye by voltage clamp technique, which yields results in terms of conductances, thus obviating the need for nonlinearity corrections. Their observations indicated that the bump rate is linearly proportional to light intensity over an intensity range of about 5 log units up to a rate of about 10⁵/s, while the conductance change due to each bump decreases in a monotonic fashion with increasing light intensity. On the other hand, the bump rate, derived from voltage measurements in Limulus eccentric cells and corrected for nonlinear summation, shows a tendency to saturate even at relatively low light intensities (Dodge et al., 1968; Wong, 1977). This tendency appears to be, at least in part, due to overcorrection for nonlinear summation (Wong, 1977). Thus, the "real" values of bump parameters, a and nT, probably lie somewhere between the uncorrected data shown in Fig. 4 and the corrected data displayed in Fig. 6, it is to be hoped, closer to Fig. 6 than Fig. 4.

Properties of Bumps at Different Light Intensities

In Limulus lateral eyes, the effective duration of bumps decreases by fourfold as light intensity increases by 5 log units (Dodge et al., 1968). In Drosophila, on the other hand, only a slight shortening of the time scale occurs in the autocovariance of receptor noise during a 3-log-unit increase in light intensity (Fig. 2),

indicating that there is only a small change in the effective duration. The difference between the two species in the magnitude of change in bump duration is also demonstrated by the frequency response measurements on the receptor potentials. If the receptor potential is a summation of randomly occurring bumps, a shorter effective duration of bumps implies a better high frequency response of the receptor potential. Whereas *Limulus* photoreceptors show a marked improvement in the high frequency response at elevated light intensity, the frequency response of the isolated receptor component of *Drosophila* electroretinogram does not change substantially with increasing light intensity (Wu and Wong, 1977).

In the intensity region below saturation of the receptor response ($\log I \leq 1$ in Figs. 3, 4, and 6), (*a*) the bump production rate shows approximately linear dependence on light intensity over more than a 3-log-unit range in intensity, and (*b*) the adjustment in the size of bumps is mainly responsible for the nonlinear dependence of the steady-state receptor potential on the light intensity (Eq. 8). In the intensity region $\log I > 1$, the bump rate shows a tendency to saturate (Figs. 4 and 6). If corrected for the error due to spontaneous bumps (see above), the above tendency would be even more striking.

It is of some interest to know the absolute bump rate at saturation, since this rate may be related to the rate-limiting step(s) in phototransduction. From Figs. 4 and 6, the bump rate is seen to saturate at about $3 \times 10^5-10^6$ bumps/s. One might now ask how much rhabdomeric membrane area is occupied by each bump at saturation. This area may be regarded as the minimum membrane area needed to support a bump. Since each bump has an effective duration of 25–30 ms, at most $2.5-3.0 \times 10^4$ bumps $\{nT$ (at saturation) $= 25-30 \times 10^{-3}$ s $\times 10^6$ bumps/s$\}$ temporally overlap at any one instant in each retinula cell at saturation. Knowing that the total rhabdomeric membrane area in each cell is approximately 9,500 μm^2 (Schinz et al., 1977), the "effective membrane area" (Wong and Knight, 1977) occupied by each bump at saturation can be calculated to be about 0.3–0.4 μm^2. This number may be compared with the average membrane area occupied by each rhodopsin molecule. The latter area may be obtained from the density of rhabdomeric membrane particles seen in freeze-fracture electron microscopy ($3.7-4.7 \times 10^3/\mu m^2$: Harris et al., 1977; Schinz et al., 1977), assuming that most of these particles are rhodopsin molecules. The average area occupied by a rhodopsin molecule turns out to be $2.1-2.7 \times 10^{-4}$ μm^2 or about three orders of magnitude smaller than the effective membrane area of the bump.

Although the mechanism(s) responsible for saturation in bump rate cannot be deduced from the present studies, it does not appear likely that depletion of visual pigment by light is directly responsible for saturation. For one thing, the receptor response exhibits saturation even when only very small fractions of the visual pigment are bleached (Pak and Lidington, 1974; Minke et al., 1975*a*). Even at saturation intensities for the bump rate (~ 1 log unit above the saturation intensity for steady-state receptor response; cf. Figs. 3, 4, and 6), we do not expect a substantial decrease in rhodopsin density under the conditions of the present experiment. Recently R. Stephenson (personal communication) of our

laboratory found that with 540-nm stimuli of saturating intensities used in these experiments, (a) rhodopsin enters into photoequilibrium with metarhodopsin within a few seconds, and (b) during photoequilibrium about 75% of the pigment is in the rhodopsin state and only 25% in the metarhodopsin state. Thus, during 540-nm stimuli of saturating intensities and 0.5-1-min durations (see Methods), there should be plenty of rhodopsin molecules available at any given instant {75% × (3.7-4.7) × 10^3 rhodopsin molecules/μm^2 × 9,500 μm^2 ≈ 3 × 10^7 rhodopsin molecules} to sustain nT greater than that found at saturation (~3 × 10^4), if the excitation of a single rhodopsin molecule is all that is needed to generate a bump. The fact that the bump rate saturates at nT of only about 3 × 10^4, or alternatively the fact that the effective membrane area of bump at saturation is many orders of magnitude larger than the average area occupied by a rhodopsin molecule suggests that it is insufficient simply to photoexcite a rhodopsin molecule to generate a bump. Some other rate-limiting steps occupying relatively large membrane areas are also involved.

REFERENCES

ADOLPH, A. R. 1964. Spontaneous slow potential fluctuations in the Limulus photoreceptor. J. Gen. Physiol. 48:297-322.

ALAWI, A. A., V. JENNINGS, J. GROSSFIELD, and W. L. PAK. 1972. Phototransduction mutants of Drosophila melanogaster. Adv. Exp. Med. Biol. 24:1-21.

ANDERSON, C. R., and C. F. STEVENS. 1973. Voltage clamp analysis of acetylcholine produced end-plate current fluctuations at frog neuromuscular junction. J. Physiol. (Lond.). 235:665-691.

BOSCHEK, C. B. 1971. On the fine structure of the peripheral retina and lamina ganglionaris of the fly, Musca domestica. Z. Zellforsch. Mikrosk. Anat. 118:369-409.

BROWN, H. M., S. HAGIWARA, H. KOIKE, and R. M. MEECH. 1970. Membrane properties of a barnacle photoreceptor examined by the voltage-clamp technique. J. Physiol. (Lond.). 208:385-413.

CONTI, F., L. J. DEFELICE, and E. WANKE. 1975. Potassium and sodium ion current noise in the membrane of the squid giant axon. J. Physiol. (Lond.). 248:45-82.

DODGE, F. A., B. W. KNIGHT, and J. TOYODA. 1968. Voltage noise in Limulus visual cells. Science (Wash. D. C.). 160:88-90.

DOWLING, J. E., and R. L. CHAPPELL. 1972. Neural organization of the median ocellus of the dragonfly. II. Synaptic structure. J. Gen. Physiol. 60:148-165.

FAIN, G. L. 1975. Quantum sensitivity of rods in the toad retina. Science (Wash. D. C.). 187:838-841.

FEIN, A., and J. S. CHARLTON. 1975. Local adaptation in the ventral photoreceptors of Limulus. J. Gen. Physiol. 66:823-836.

FUORTES, M. G. F., and S. YEANDLE. 1964. Probability of occurrence of discrete potential waves in the eye of Limulus. J. Gen. Physiol. 47:443-463.

Hagins, W. A. 1965. Electrical signs of information flow in photoreceptors. *Cold Spring Harbor Symp. Quant. Biol.* **30:**403–418.

Harris, W. A., D. F. Ready, E. D. Lipson, A. J. Hudspeth, and W. S. Stark. 1977. Vitamin A deprivation and *Drosophila* photopigments. *Nature (Lond.)* **266:**648–650.

Katz, B., and R. Miledi. 1972. The statistical nature of the acetylcholine potential and its molecular components. *J. Physiol. (Lond.)*. **224:**665–699.

Kirschfeld, K. 1966. Discrete and graded receptor potentials in the compound eye of the fly (*Musca*). *In* The Functional Organization of the Compound Eye. C. G. Bernhard, editor. Pergamon Press Ltd., Oxford. 291–307.

Kirschfeld, K. 1972. The visual system of *Musca:* Studies on optics, structure and function. *In* Information Processing in the Visual System of Arthropods. R. Wehner, editor. Springer-Verlag K. G., Berlin. 61–74.

Knight, B. W. 1972. Some point processes in motor and sensory neurophysiology. *In* Stochastic Point Processes. P. A. W. Lewis, editor. John Wiley & Sons, Inc., New York. 732–755.

Lindsley, D. L., and E. H. Grell. 1968. Genetic Variations of *Drosophila melanogaster*. Carnegie Institution of Washington, Washington, D. C. 266 pp.

Martin, A. R. 1966. Quantal nature of synaptic transmission. *Physiol. Rev.* **46:**51–66.

Millecchia, R., and A. Mauro. 1969a. The ventral photoreceptor cells of *Limulus*. II. The basic photoresponse. *J. Gen. Physiol.* **54:**310–330.

Millecchia, R., and A. Mauro. 1969b. The ventral photoreceptor cells of *Limulus*. III. A voltage-clamp study. *J. Gen. Physiol.* **54:**331–351.

Minke, B., C-F., Wu, and W. L. Pak. 1975a. Induction of photoreceptor voltage noise in the dark in *Drosophila* mutant. *Nature (Lond.)*. **258:**84–87.

Minke, B., C-F. Wu, and W. L. Pak. 1975b. Isolation of light-induced responses of the central retinula cells from the electroretinogram of *Drosophila. J. Comp. Physiol.* **98:**345–355.

Muller, K. J. 1973. Photoreceptors in the crayfish compound eye: Electrical interactions between cells as related to polarized-light sensitivity. *J. Physiol. (Lond.)*. **232:**573–595.

Naka, K., and W. A. H. Rushton. 1966. S-potentials from colour units in the retina of fish *Cyprinidae. J. Physiol. (Lond.)*. **185:**536–555.

Pak, W. L. 1975. Mutations affecting the vision of *Drosophila melanogaster*. *In* Handbook of Genetics. R. C. King, editor. Plenum Publishing Corp., New York. **3:**703–733.

Pak, W. L., and K. J. Lidington. 1974. Fast electrical potential from a long-lived, long-wavelength photoproduct of fly visual pigment. *J. Gen. Physiol.* **63:**740–756.

Pak, W. L., S. E. Ostroy, M. C. Deland, and C-F. Wu. 1976. Photoreceptor mutant of *Drosophila*: Is protein involved in intermediate steps of phototransduction? *Science (Wash. D. C.)*. **194:**956–959.

Rice, S. O. 1944. Mathematical analysis of random noise. *In* Selected Papers on Noise and Stochastic Processes. 1954. N. Wax, editor. Dover Publications, Inc., New York. 133–294.

Rushton, W. A. H. 1961. The intensity factor in vision. *In* Light and Life. W. D. McElroy and H. B. Glass, editors. The Johns Hopkins University Press, Baltimore. 706–723.

Schinz, R., S. E. Ostroy, and W. L. Pak. 1977. Freeze-fracture study of the *Drosophila* rhabdomeric membrane. The Association for Research in Vision and Ophthalmology Abstracts. 146, no. 1. (Abstr.)

Scholes, J. 1965. Discontinuity of the excitation process in locust visual cells. *Cold Spring Harbor Symp. Quant. Biol.* **30:**517–527.

SHAW, S. R. 1969. Interreceptor coupling in ommatidia of drone honeybee and locust compound eyes. *Vision Res.* **9**:999–1029.

SIMON, E. J., T. D. LAMB, and A. L. HODGKIN. 1975. Spontaneous voltage fluctuations in retinal cones and bipolar cells. *Nature (Lond.).* **256**:661–662.

SMITH, T. G., F. BAUMANN, and M. G. F. FUORTES. 1965. Electrical connections between visual cells in the ommatidium of *Limulus. Science (Wash. D. C.).* **147**:1446–1448.

SREBRO, R., and M. BEHBEHANI. 1972. Light adaptation of discrete waves in the *Limulus* photoreceptor. *J. Gen. Physiol.* **60**:86–101.

STEVENS, C. F. 1976. A comment on Martin's relation. *Biophys. J.* **16**:891–895.

TRUJILLO-CENÓZ, O. 1965. Some aspects of the structural organization of the intermediate retina of dipterans. *J. Ultrastruct. Res.* **13**:1–33.

WONG, F. 1977. Mechanisms of the phototransduction process in invertebrate photoreceptors. Ph.D. thesis. The Rockefeller University, New York.

WONG, F., and B. W. KNIGHT. 1977. The adapting-bump model in *Limulus* ventral photoreceptors. The Association for Research in Vision and Ophthalmology Abstracts. 119, no. 2. (Abstr.)

WU, C-F., and W. L. PAK. 1975. Quantal basis of photoreceptor spectral sensitivity of *Drosophila melanogaster. J. Gen. Physiol.* **66**:149–168.

WU, C-F., and F. WONG. 1977. Frequency characteristics in the visual system of *Drosophila*: Genetic dissection of electroretinogram components. *J. Gen. Physiol.* **69**:705–724.

YEANDLE, S. 1957. Studies on the slow potentials and the effects of cations on the electrical responses of the *Limulus* ommatidium. Ph.D. thesis. The Johns Hopkins University, Baltimore.

ZETTLER, F., and M. JÄRVILEHTO. 1973. Active and passive axonal propagation of nonspike signals in the retina of *Calliphora. J. Comp. Physiol.* **85**:89–104.